



## Applications of a shadow camera system for energy meteorology

Pascal Kuhn<sup>1</sup>, Stefan Wilbert<sup>1</sup>, Christoph Prah<sup>1</sup>, Dominik Garsche<sup>1</sup>, David Schüler<sup>1</sup>, Thomas Haase<sup>1</sup>, Lourdes Ramirez<sup>2</sup>, Luis Zarzalejo<sup>2</sup>, Angela Meyer<sup>3</sup>, Philippe Blanc<sup>4</sup>, and Robert Pitz-Paal<sup>5</sup>

<sup>1</sup>German Aerospace Center (DLR), Institute of Solar Research, Plataforma Solar de Almería, Ctra. De Senés s/n km 5, 04200 Tabernas, Spain

<sup>2</sup>CIEMAT, Energy Department – Renewable Energy Division, Av. Complutense, 40, 28040 Madrid, Spain

<sup>3</sup>MeteoSwiss, Les Innuardes, 1530 Payerne, Switzerland

<sup>4</sup>MINES ParisTech, PSL Research University, O. I. E. Centre Observation, Impacts, Energy, CS 10207, 06904, Sophia Antipolis CEDEX, France

<sup>5</sup>German Aerospace Center (DLR), Institute of Solar Research, Linder Höhe, 51147 Cologne, Germany

**Correspondence:** Pascal Kuhn (pascal.kuhn@dlr.de)

Received: 10 November 2017 – Accepted: 9 January 2018 – Published: 13 February 2018

**Abstract.** Downward-facing shadow cameras might play a major role in future energy meteorology. Shadow cameras directly image shadows on the ground from an elevated position. They are used to validate other systems (e.g. all-sky imager based nowcasting systems, cloud speed sensors or satellite forecasts) and can potentially provide short term forecasts for solar power plants. Such forecasts are needed for electricity grids with high penetrations of renewable energy and can help to optimize plant operations. In this publication, two key applications of shadow cameras are briefly presented.

### 1 Introduction

The variable nature of the solar resource challenges the stability of electricity grids with high solar penetrations. Besides storage, irradiance forecasts are means to cope with these fluctuations and the combination of both technologies will most likely ensure future grid stability. Intra-hour variations of the solar resource are mainly caused by transient clouds. Due to limitations of spatial and temporal resolutions, shading events on industrial solar power plants are hard to predict using satellite based forecasts. Very short term forecasts, e.g. for the next 15 min, can be provided by camera based nowcasting systems (Chow et al., 2011; Kuhn et al., 2017b).

To the best of our knowledge, all camera based nowcasting systems so far are based on upward-facing all-sky imagers, taking images of the sky above the camera. In these all-sky images, clouds are detected. From a series of images from multiple all-sky imagers, several attributes (cloud

height, cloud speed, cloud movement direction, cloud transmittance, cloud dynamics, etc.) are assigned to the clouds (see e.g. Chow et al., 2011; Yang et al., 2014). With these attributes and considering a ground model, shadows are projected and spatially resolved irradiance maps are generated (see e.g. Nouri et al., 2017).

In this paper, a novel approach for camera based nowcasting systems is presented. This approach is based on downward-facing cameras (“shadow cameras”) that take images of the ground from an elevated position. In these images, the brightness of the ground as influenced by cloud shadows can be seen and converted to cloud shadow and irradiance maps (Kuhn et al., 2017a). Furthermore, the application of a shadow camera system for the validation of all-sky imager based nowcasting systems is discussed.

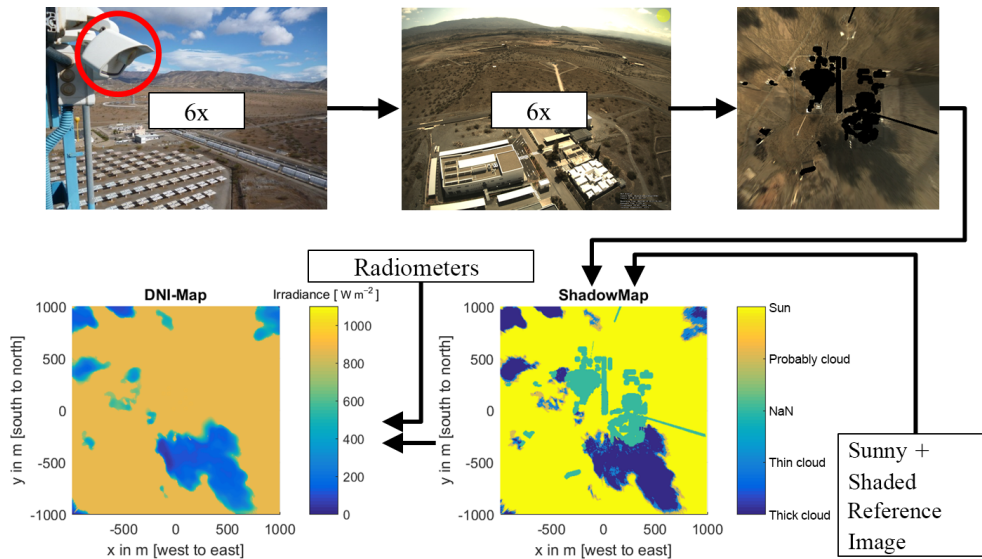


**Figure 1.** Working principle of the shadow camera system. Downward-facing cameras are used to generate spatially resolved irradiance (DNI, GHI, GTI) maps.

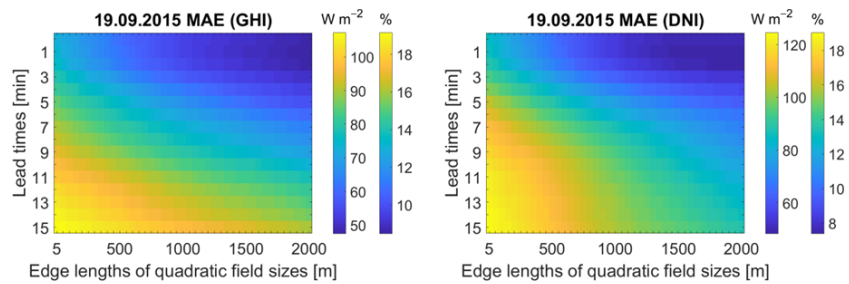


**Figure 2.** Absolute and relative mean absolute error of the WobaS-4cam system for GHI and DNI for various lead times and field sizes.

## 2 The shadow camera system

### 2.1 Working principle and methodology

At the Plataforma Solar de Almería, a novel shadow camera system is installed. Figure 1 visualizes the working principle of the shadow camera system: The system uses the inputs of six downward facing cameras placed on an 87 m high tower (CIEMAT CESA-I, Fig. 1, top left). The cameras take images of the ground every 15 s, which are then combined into an undistorted orthoimage (Fig. 1, top middle and right). The orthoimages have a spatial resolution of 5 m × 5 m and image an area of 4 km<sup>2</sup>. By comparing the current orthoimage with two reference orthoimages, taken when no shadow fell on the imaged area (“sunny reference”) and taken when the whole area was shaded (“shaded reference”), shadows are segmented. For unshaded areas in the current orthoimage, clear sky irradiance values are taken as modelled from ground measurements. The irradiances (DNI – Direct Normal Irradiance, GHI – Global Horizontal Irradiance, GTI – Global Tilted Irradiance) for the shaded areas are

derived from pixel intensities of the current orthoimage relative to normalized pixel intensities of the reference orthoimages. The shadow camera system is presented and validated in Kuhn et al. (2017a). Comparing pixels of the irradiance maps to corresponding ground measurements for one-minute temporal averages, the shadow camera system shows deviations of RMSE (DNI) between 4.2 and 16.7 % and RMSE (GHI) deviations below 10 %.

### 2.2 Studying spatial aggregation effects on nowcasted irradiance maps

Using the spatially resolved irradiance maps provided by the shadow camera system, nowcasted irradiance maps generated by all-sky imager based nowcasting systems can be validated with special focus on spatial aggregation effects. Figure 2 depicts the mean absolute error (MAE) for GHI and DNI of the WobaS-4cam nowcasting system. The WobaS-4cam system uses the inputs of four all-sky imagers and is described in (Nouri et al., 2017). The irradiance maps produced by WobaS-4cam for lead times between 0 and 15 min

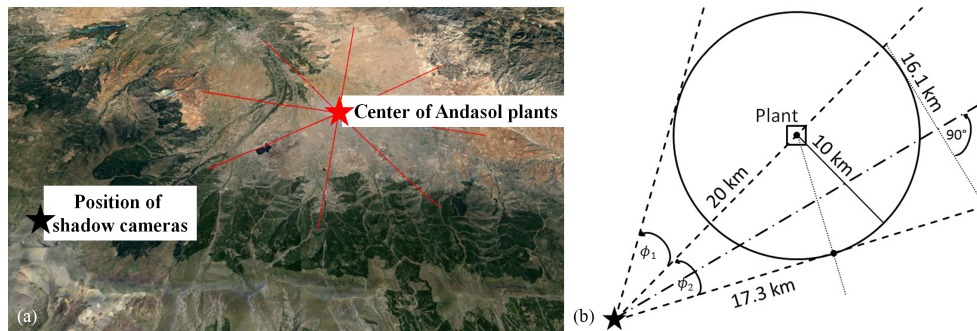


**Figure 3.** Case study of a potential shadow camera based nowcasting system for the Andasol solar power plants in Spain. (a) Red lines mark 10 km distances around the plants' centre. (Google Earth) (b) Geometry and distances. The cameras' hypothetical position ( $37^{\circ}7'27.15''$  N,  $3^{\circ}15'6.72''$  W) is marked with a star.

are compared to the reference irradiance maps of the shadow camera system for field sizes between  $5\text{ m} \times 5\text{ m}$  (one pixel) and  $4\text{ km}^2$ . Unsurprisingly, longer lead times lead to larger deviations (Kuhn et al., 2017c). However, these deviations shrink significantly if spatial aggregation effects are considered. Industrial photovoltaic (PV) plants cover areas of several  $\text{km}^2$  and the single most important parameter to predict is the average irradiance over the whole plant. Thus, these spatial aggregation effects are inherently present and play a major role for the validation of nowcasting systems (Kuhn et al., 2017d).

### 2.3 Case study of a potential shadow camera based nowcasting system

As shown in Sect. 2.1, shadow camera systems generate highly spatially resolved shadow and irradiance maps. By tracking cloud shadows, e.g. with the differential approach introduced in Kuhn et al. (2017e, f), future shadow positions can be estimated. The shadow camera system used for the validation presented in the previous section is located on an 87 m high tower and can thus only image a relatively small area of  $4\text{ km}^2$ . In this section, the potential application of such a system for the Andasol solar power plants (Andasol 1–3,  $50\text{ MW}_{\text{el}}$  each) is discussed.

If nowcasts with lead times up to 10 min are required and if cloud speeds up to  $60\text{ km h}^{-1}$  ( $16.7\text{ m s}^{-1}$ ) are considered, the required imaged area around the plants must be at least 10 km in every direction. A maximum considered speed of  $16.7\text{ m s}^{-1}$  is reasonable as the mean cloud speed in this region is  $7.36\text{ m s}^{-1}$  and the median speed is  $6.67\text{ m s}^{-1}$  (Kuhn et al., 2017e). Under otherwise unchanged conditions, greater lead times can be achieved by using more and distributed cameras.

In Fig. 3, the topographical situation for the Andasol plants is outlined: Two shadow cameras could potentially be located on a mountain approximately 20 km away from and 2 km above the plants. The maximum required range of vision is thus 30 km, which is realistic in this region (Hanrieder

et al., 2015). We consider using 6 MegaPixel cameras with a viewing angle of  $30^{\circ}$ . This results in an area element of  $8\text{ m} \times 17\text{ m}$  for the pixel the farthest away. If higher spatial resolutions are needed, cameras with higher resolutions or more cameras with a smaller field of view could be used.

## 3 Conclusion

In this publication, a short overview of the applications of shadow cameras is given. Shadow cameras provide references for all-sky imager based nowcasting systems, helping to understand spatial aggregation effects inherently present in industrial PV plants. Moreover, a case study of a hypothetical shadow camera based nowcasting system for the three Andasol solar power plants is performed, revealing very promising potentials.

**Data availability.** Data of the shadow camera system can be made accessible upon request.

**Competing interests.** The authors declare that they have no conflict of interest.

**Special issue statement.** This article is part of the special issue “17th EMS Annual Meeting: European Conference for Applied Meteorology and Climatology 2017”. It is a result of the EMS Annual Meeting: European Conference for Applied Meteorology and Climatology 2017, Dublin, Ireland, 4–8 September 2017.

**Acknowledgements.** The research presented in this publication has received funding from the European Union's Horizon 2020 programme for the initial development of the shadow camera system (PreFlexMS, Grant Agreement no. 654984). With founding from the German Federal Ministry for Economic Affairs and Energy within the WobaS project, the generation of irradiance maps was implemented. The European Union's FP7 programme

under Grant Agreement no. 608623 (DNICast project) financed operations of all-sky imagers and other ground measurements. Thanks to the colleagues from the Solar Concentrating Systems Unit of CIEMAT for the support provided in the installation and maintenance of the shadow cameras. These instruments are installed on CIEMAT's CESA-I tower of the Plataforma Solar de Almería.

Edited by: Sven-Erik Gryning

Reviewed by: Manajit Sengupta and one anonymous referee

## References

- Chow, C. W., Urquhart, B., Lave, M., Dominguez, A., Kleissl, J., Shields, J., and Washom, B.: Intra-hour forecasting with a total sky imager at the UC San Diego solar energy testbed, *Sol. Energy*, 85, 2881–2893, doi.org/10.1016/j.solener.2011.08.025, 2011.
- Hanrieder, N., Wilbert, S., Pitz-Paal, R., Emde, C., Gasteiger, J., Mayer, B., and Polo, J.: Atmospheric extinction in solar tower plants: absorption and broadband correction for MOR measurements, *Atmos. Meas. Tech.*, 8, 3467–3480, https://doi.org/10.5194/amt-8-3467-2015, 2015.
- Kuhn, P., Wilbert, S., Prah, C., Schüler, D., Haase, T., Hirsch, T., Wittmann, M., Ramirez, L., Zarzalejo, L., Meyer, A., Vuilleumier, L., Blanc, P., and Pitz-Paal, R.: Shadow camera system for the generation of solar irradiance maps, *Sol. Energy*, 157, 157–170, doi.org/10.1016/j.solener.2017.05.074, 2017a.
- Kuhn, P., Nouri, B., Wilbert, S., Schmidt, T., Prah, C., Yasser, Z., Ramirez, L., Zarzalejo, L., Meyer, A., Vuilleumier, L., Blanc, P., and Pitz-Paal, R.: Validation of an All Sky Imager based nowcasting system for industrial PV plants, *Prog. Photovoltaics Res. Appl.*, 1–14, https://doi.org/10.1002/pip.2968, 2017b.
- Kuhn, P., Wilbert, S., Schüler, D., Prah, C., Haase, T., Ramirez, L., Zarzalejo, L., Meyer, A., Vuilleumier, L., Blanc, P., Dubrana, J., Kazantzidis, A., Schroedter-Homscheidt, M., Hirsch, T., and Pitz-Paal, R.: Validation of Spatially Resolved All Sky Imager Derived DNI Nowcasts, *Aip. Conf. Proc.*, 1850, 140014, https://doi.org/10.1063/1.4984522, 2017c.
- Kuhn, P., Wilbert, S., Prah, C., Kazantzidis, A., Ramirez, L., Zarzalejo, L., Vuilleumier, L., Blanc, P., and Pitz-Paal, R.: Validation of nowcasted spatial DNI maps, *DNICast Deliverable 4.1*, available at: <http://www.dnicast-project.net/> (9 February 2018), 2017d.
- Kuhn, P., Wirtz, M., Wilbert, S., Bosch, J. L., Wang, G., Heinemann, D., and Pitz-Paal, R.: Field validation and benchmarking of a cloud shadow speed sensor, *Sol. Energy*, in review, 2017e.
- Kuhn, P., Wirtz, M., Killius, N., Wilbert, S., Bosch, J. L., Hanrieder, N., Nouri, B., Kleissl, J., Schroedter-Homscheidt, M., Heinemann, D., Kazantzidis, A., Blanc, P., and Pitz-Paal, R.: Benchmarking three low-cost, low-maintenance cloud height measurement systems, *Sol. Energy*, in review, 2017f.
- Nouri, B., Kuhn, P., Wilbert, S., Prah, C., Pitz-Paal, R., Blanc, P., Schmidt, T., Yasser, Z., and Ramirez, L.: Short term nowcasting system for temporal and spatial resolved DNI maps based on individual three dimensional cloud objects, *SolarPACES 2017*, 2017.
- Yang, H., Kurtz, B., Nguyen, D., Urquhart, B., Chow, C. W., Ghonima, M., and Kleissl, J.: Solar irradiance forecasting using a ground-based sky imager developed at UC San Diego, *Sol. Energy*, 103, 502–524, doi.org/10.1016/j.solener.2014.02.044, 2014.